

Self-assembling chitosan based injectable and expandable sponge with antimicrobial property for hemostasis and wound healing

Shujun Cao ^a, Peihong Ji ^a, Lili Hao ^a, Chao Sun ^{b,*}, Hongli Mao ^{a,*}, Zhongwei Gu ^a

^a Research Institute for Biomaterials, Tech Institute for Advanced Materials, Bio-inspired Biomedical Materials & Devices Center, College of Materials Science and Engineering, Jiangsu Collaborative Innovation Center for Advanced Inorganic Function Composites, Suqian Advanced Materials Industry Technology Innovation Center, Nanjing Tech University, Nanjing 211816, China

^b Department of Spine Surgery, The Affiliated Jiangning Hospital of Nanjing Medical University, Nanjing 211100, China

ARTICLE INFO

Keywords:

Chitosan
Injectable
Shape memory
Sponge
Hemostasis
Wound healing

ABSTRACT

Chitosan and chitosan derivative are widely used in hemostasis, antibiosis and wound repair for its good biocompatibility and unique effect. However, the preparation of chitosan based hemostatic materials or wound dressings generally involves chemical crosslinking agent introduction, acid residue or complicated preparation process, which limits its clinical application. In this study, an injectable and expandable chitosan sponge was constructed by chitosan (CS) and quaternized chitosan (QCS) self-assembly without acid retention and chemical crosslinker introduction. In the neutral condition, the hydrogen bond of CS molecules can act as the driving force to form cross-linking network, and the QCS was introduced to regulate the hydrogen bond of CS to avoid the excessive aggregation. The porous QCS/CS sponge was obtained by freeze-drying of the self-assembly QCS/CS hydrogel. The sponge exhibited high expansibility, injectability and water/blood triggered shape memory property. Due to the introduction of QCS, the sponge showed good antibacterial properties, which can protect the wound from bacterial invasion. The convenient and green preparation method of injectable and expandable QCS/CS sponge is a potential method for the treatment of hemostasis and wound healing.

1. Introduction

Acute hemorrhage caused by accidents and surgery is easy to lead excessive blood loss and bacterial infection, threatening life's safety (Lu et al., 2022; Zhao et al., 2024). At present, gauze and bandages are the commonly used materials in clinical hemostasis (Peng et al., 2023). However, those hemostatic dressing is difficult to reach deep wounds, and has poor degradability, hemostatic and antibacterial properties. Expandable hemostatic sponge is a kind of hemostatic material with good absorptive capacity and controllable volume (Marani & Ehtesabi, 2023). The sponge can be easily transported into wound and plays a role by rapid expansion. So, the development of expandable sponges with good biodegradability, blood coagulability and antibacterial properties has broad prospect in hemostasis (Zhao et al., 2021).

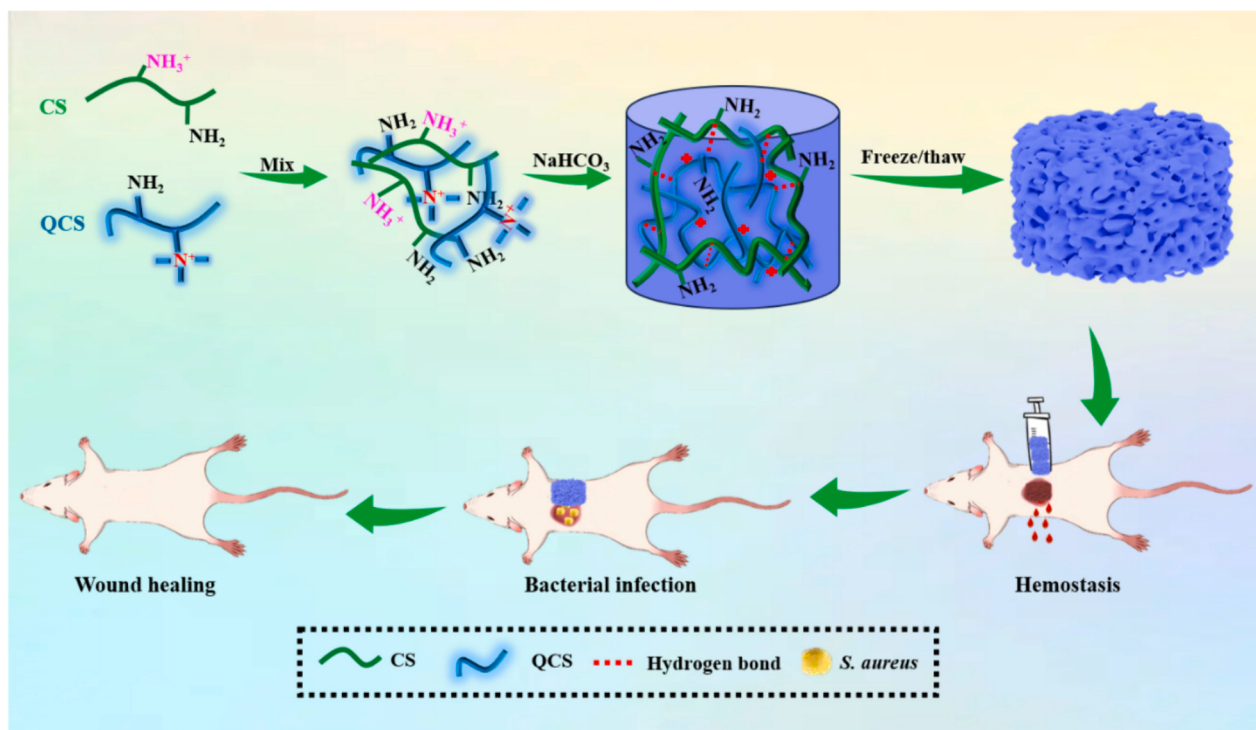
Due to the high physicochemical activity and biocompatibility of chitosan (CS), the CS based expandable sponge exhibits obvious advantages in hemostasis and wound healing promotion (Liu et al., 2022; Zhang et al., 2024). However, there are still some issues in the application of CS based expandable sponge, such as complex preparation

process, or adverse stimulation caused by residual acid and chemical crosslinking agents (Gao et al., 2022, 2023a; Liu et al., 2023). In order to reduce the stimulation caused by acid and enhance the stability of the CS based sponge, Jin et al. prepared the acid-removed chitosan sponge by soaking the acidic chitosan sponge in the alkaline solution (Jin et al., 2023). Unfortunately, with the acid removing from CS sponge, the attractive force between the molecular chains of CS increases rapidly, which can lead to the shrinking and entanglement of CS molecular, causing a decline in the water absorption and expandability (Z.T. Li et al., 2024; Wang et al., 2023). In addition, the acidity removal of CS ($\text{pH} > 6.5$) can lead to its antibacterial decrease or disappear (Juan et al., 2022; Mottaghitalab et al., 2024; Priddy-Arrington et al., 2023). For retaining the high expansibility of CS sponge, researchers added glutaraldehyde into CS solution in the preparation process, followed by freeze-drying and soaking in alkaline solution to remove excess acid (Ahmad et al., 2024; Yao et al., 2022). But the volume of prepared CS sponge still reduces uncontrollably (Luo et al., 2022).

In order to maintain the high expansion capacity, recent studies have been conducted by neutralizing the acidity of chitosan in solution (Qi

* Corresponding authors.

E-mail addresses: drsunchao@163.com (C. Sun), h.mao@njtech.edu.cn (H. Mao).



Scheme 1. Schematic diagram of the design strategy of QCS/CS sponge as a versatile biomedical dressing for rapid hemostasis and wound healing.

et al., 2023a,b). After neutralizing the acidity, a stable and dispersed CS solution can be formed by breaking the aggregation through high-speed homogenizer, and epichlorohydrin (ECH) was further introduced to crosslink the CS to form a stable structure with sufficient chemical crosslinking. The preparation process avoids the appearance of gelation and removes the acidity, preserving the high expansibility of the CS based sponge. Therefore, neutralizing the acidity of CS in solution to prepare expandable sponge is an efficient method. However, there are still great challenges in enhancing antibacterial properties and reducing the use of chemical crosslinkers. Chitosan derivative such as quaternary ammonium (QCS) shows good biocompatibility and antibacterial properties (Liang et al., 2023; Qiao et al., 2023; Yang et al., 2021). The introduction of charged polysaccharide into the CS is expected to play an important role.

Inspired by previous studies, a novel injectable and expandable QCS/CS sponge with good antibacterial ability was developed for hemostasis and wound healing. The QCS/CS sponge was prepared following Scheme 1. By neutralizing the acidity of CS in solution and introducing QCS to regulate the hydrogen bond of CS to avoid the precipitation, a cross-linking network formed between CS and QCS/CS hydrogel was prepared through hydrogen bond self-assembly. QCS/CS sponge was obtained through freeze-drying. The experimental results showed that the prepared QCS/CS sponge has excellent shape memory properties and high expansion rate. Compared with gauze and gelatin sponge, QCS/CS sponge exhibited better blood cell adhesion and clotting ability. In addition, the prepared QCS/CS sponge can effectively kill *S. aureus* and *E. coli* to avoid bacterial infection. The results of rat liver injury model showed that QCS/CS sponge can effectively fill the wound and stop bleeding quickly. All the results demonstrate that the QCS/CS sponge is an appropriate candidate for the treatment of deep acute hemorrhage and wound healing.

2. Materials and methods

2.1. Materials

Chitosan (CS, Deacetylation ≥95 %, MW = 500,000) and Sodium

bicarbonate (NaHCO₃) was purchased from Macklin Co., Ltd. Glycidyl trimethylammonium chloride (GTMAC) were obtained from Macklin Co., Ltd. mouse NIH 3T3 fibroblasts were purchased from Shanghai Institutes for Biological Sciences. All animal research was carried out by the National Research Council's Guide for the Care and Use of Laboratory Animals and was authorized by Nanjing Tech University's animal experimentation ethical committee. SD rats (5–6 weeks old, 150–200 g, male) were purchased from the Nanjing Qinglongshan Animal Breeding Co., Ltd.

2.2. Methods

2.2.1. Fabrication of QCS/CS sponge

QCS was prepared according to previous reports (Z.T. Li et al., 2024). A certain amount of CS was dissolved in 15 mL acetic acid aqueous solution to obtain CS solution. Then, 2 wt% QCS solution was added to the CS solution and stirred at room temperature, and the mass ratio of QCS to CS was 1:1, 1:1.25, 1:1.5, 1:1.75. Following, 0.147, 0.147, 0.221 and 0.294 g NaHCO₃ was added to QCS/CS solution. After stirring, the sponge precursor was transferred to the mold and reacted at -20 °C for 24 h. Then, the obtained sponge was thawed at room temperature, and the sponge was soaked in DI water for 2–3 days to remove excess CS, QCS, NaHCO₃. Finally, the QCS/CS sponges were obtained by freeze-dried. The sponges were named QCS/CS₁, QCS/CS₂, QCS/CS₃ and QCS/CS₄.

2.3. Characterization

Scanning electron microscopy (SEM, Philips XL 30 FEG, USA) was adopted to observe the morphologies of QCS/CS sponges. Fourier transform infrared spectroscopy (FT-IR, Bruker VERTEX70, Germany) was used to study the chemical functional groups of sponge.

2.4. Molecular dynamics simulation

The partial charge of CS and QCS molecule was calculated using Gaussian 16 code and the 6-311 g (d, p) basis functions were applied.

The aggregation behavior of CS and QCS in aqueous solution was studied by molecular dynamics simulation. The details of molecular dynamics simulation are in the supplementary material.

2.5. Measurements and evaluations of QCS/CS sponge

2.5.1. Porosity

The pre-weighed sponge (W_1) was immersed in ethanol, placed in a vacuum glass drying dish for 10 min, and then taken out and weighed (W_2). The porosity was obtained by the formula (1):

$$P (\%) = \frac{W_2 - W_1}{\rho \times V_1} \times 100\% \quad (1)$$

ρ is the density of ethanol; V_1 is the volume of sponges.

2.5.2. Swelling ratio

The weighed sponge (W_a) was soaked in PBS solution for 24 h, then the PBS was discarded, and the excess liquid on the surface of the sponge was gently wiped with filter paper and weighed (W_b). The Swelling ratio was obtained by the formula (2):

$$\text{Swelling ratio (\%)} = \frac{W_b - W_a}{W_a} \times 100\% \quad (2)$$

2.5.3. Shape memory and mechanical properties

The compression properties of sponges were tested by a rheometer (DHR-1, TA, USA). The compression rate is set to 1 mm/s. Sponge ($D = 13$ mm) was immersed in PBS and then compressed at 75 % deformation. For the cyclic compression test, sponge was immersed in PBS and then cycled 5 times with a compression strain of 75 %.

2.5.4. Antibacterial activity

First, 100 μ L bacterial suspension (10^6 CFU/mL) was co-incubated with different group sponge (10 mg) for 4 h, and the bacteria suspension was diluted by a certain time with PBS. Subsequently, 10 μ L bacterial suspension was evenly smeared on LB agar plate and place in the incubator for 24 h. Finally, take photos of the culture plate. *S. aureus* (ATCC 29213) and *E. coli* (ATCC 8739) without sponge were used as control groups to evaluate the antibacterial activity of sponge.

50 μ L bacterial solution (10^6 CFU/mL) was dropped on the sponge, incubated at 37 °C for 4 h, and then 950 μ L LB liquid medium was added to sponge. The 200 μ L bacterial solution was transferred to the 96-well plate and OD600 was measured by Microplate reader. The group containing only bacterial solution and medium was set as the control group. The antibacterial rate is calculated according to formula (3):

$$\text{The antibacterial rate (\%)} = \frac{OD_{control} - OD_{sponge}}{OD_{control}} \times 100\% \quad (3)$$

2.5.5. Blood absorption ratio

The weighed sponge (W_a) was soaked in blood for 24 h, then the blood was discarded, and the excess blood on the surface of the sponge was gently wiped with filter paper and weighed (W_b). The blood absorption ratio was obtained by the formula (4):

$$\text{Blood absorption ratio (\%)} = \frac{W_2 - W_1}{W_1} \times 100\% \quad (4)$$

2.5.6. Hemolysis ratio

The hemolysis ratio of QCS/CS sponge was carried out according to previous reports with some modifications (Z.T. Li et al., 2024), as detailed in the Supporting Information.

2.5.7. Red blood cell adhesion

The red blood cell adhesion (RBC) rate of QCS/CS sponge was carried out according to previous reports with some modifications (P.X. Zhao et al., 2023), as detailed in the Supporting Information.

Take a certain volume of blood drops in QCS/CS sponge and incubate at 37 °C for 5 min. Then, the blood cells on the sponge were immobilized with 2.5 % glutaraldehyde and dehydrated with graded concentrations of ethanol (25 %, 50 %, 75 %, 95 %, and 100 %). Finally, after freeze-drying, the adhesion of blood cells on QCS/CS then was observed by SEM.

2.5.8. Blood clotting index

The blood clotting index (BCI) of QCS/CS sponge was carried out according to previous reports with some modifications, as detailed in the Supporting Information.

2.5.9. Cell proliferation and cytotoxicity

The cell proliferation and cytotoxicity of sponge were carried out according to previous reports with some modifications (Cao et al., 2023b), as detailed in the Supporting Information.

2.5.10. Hemostatic performance *in vivo*

The hemostatic ability of QCS/CS sponge was evaluated by the liver prick injury model and liver noncompressible hemorrhage model. SD rats were randomly divided into 3 groups with 5 rats in each group: the control group (no treatment after bleeding), gelatin sponge group, and QCS/CS sponge.

In the rat liver prick injury model, anesthetized rats were fixed to the operating table, and exposed to the liver. A syringe was used to stab the surface of the liver, and the sample was immediately pasted to the wound until the bleeding stopped. Then, the blood loss and hemostasis time were recorded.

In the rat liver noncompressible hemorrhage model, a biopsy instrument with a diameter of 5 mm was used to create the liver hemorrhage, and the sample was immediately injected into the wound until the bleeding stopped. Then, the blood loss and hemostasis time were recorded.

2.5.11. Wound healing properties *in vivo*

Ordinary SD rats were randomly divided into three groups as control group, gelatin sponge group and QCS/CS sponge group. A wound with a diameter of 1.5 cm was created and infected with a 10^8 CFU/mL *S. aureus* suspension (200 μ L) to establish an infectious wound model. In the control group without any treatment, and the commercial gelatin sponge group and the QCS/CS sponge group were placed at the wound site and fixed, respectively. Wound photos were taken on 0, 7th, and 12th, and the regenerated tissues were taken out for H&E staining to further observe the tissue growth. The wound closure ratio was obtained by the formula (5):

$$\text{Wound closure ratio (\%)} = \frac{\text{Area}_{0 \text{ day}} - \text{Area}_{n \text{ day}}}{\text{Area}_{0 \text{ day}}} \times 100\% \quad (5)$$

2.5.12. *In vivo* biodegradability performance

Sterile QCS/CS sponge was implanted subcutaneously into the back of SD rats and the wound was sutured. The sponge, surrounding tissue, and skin were removed at the 1 week and 3 weeks, respectively. H&E staining was used to observe the degradation degree and histomorphology changes of sponge.

2.6. Statistical analysis

All data are represented as means \pm SDs, Statistical analysis was performed in GraphPad Prism 7.0 and by one-way ANOVA, and $*P < 0.05$, $**P < 0.01$, and $***P < 0.001$ were considered statistically significant.

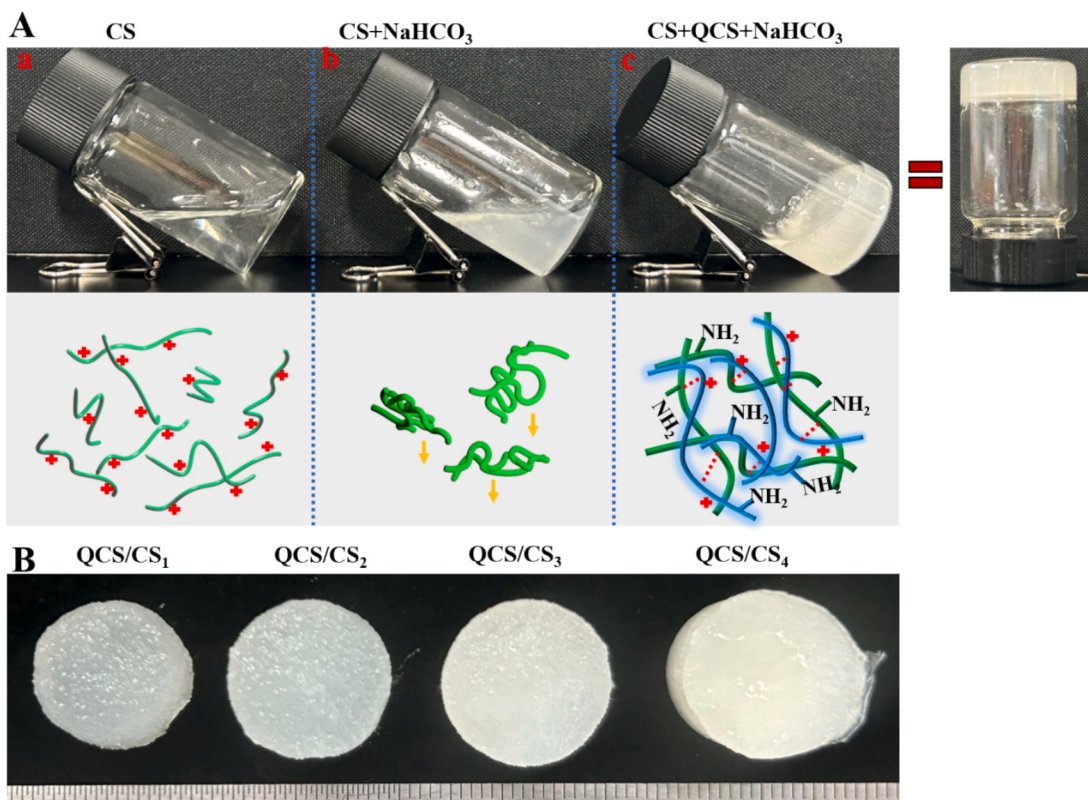


Fig. 1. (A) Gelation mechanism of QCS/CS; (B) Digital photo of QCS/CS sponge.

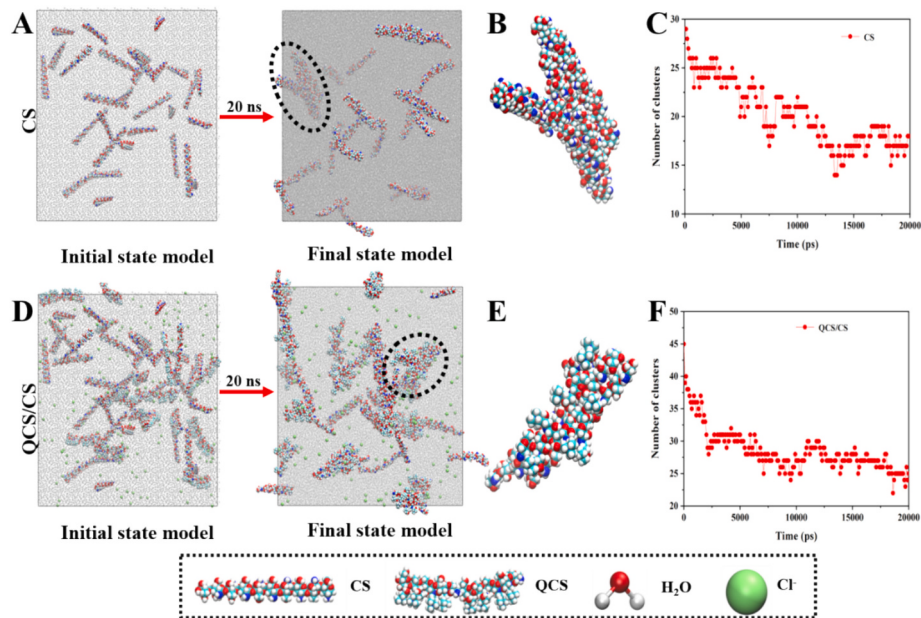


Fig. 2. (A) The initial and final state model of CS was simulated; (B) Simulate the largest cluster structure in CS; (C) The number of clusters of CS molecules formed in the simulated system; (D) The initial and final state model of QCS/CS was simulated; (E) Simulate the largest cluster structure in QCS/CS; (F) The number of clusters of QCS/CS molecules formed in the simulated system.

3. Results and discussion

3.1. Preparation of QCS/CS sponge

Under acidic conditions, the amino group of CS is protonated and the solubility of CS in aqueous solution increases (Fig. 1A-a). Under neutral

or alkaline conditions, CS is deprotonated and the intermolecular hydrogen bond is enhanced, resulting in the aggregation and precipitation of CS molecules (Fig. 1A-b). Based on above studies, QCS was introduced to regulate the hydrogen bond of CS. QCS can form hydrogen bond with CS to reduce the effect of intermolecular hydrogen bond of CS to avoid precipitation (Fig. 1A-c). Hydrogen bond between CS acted as a

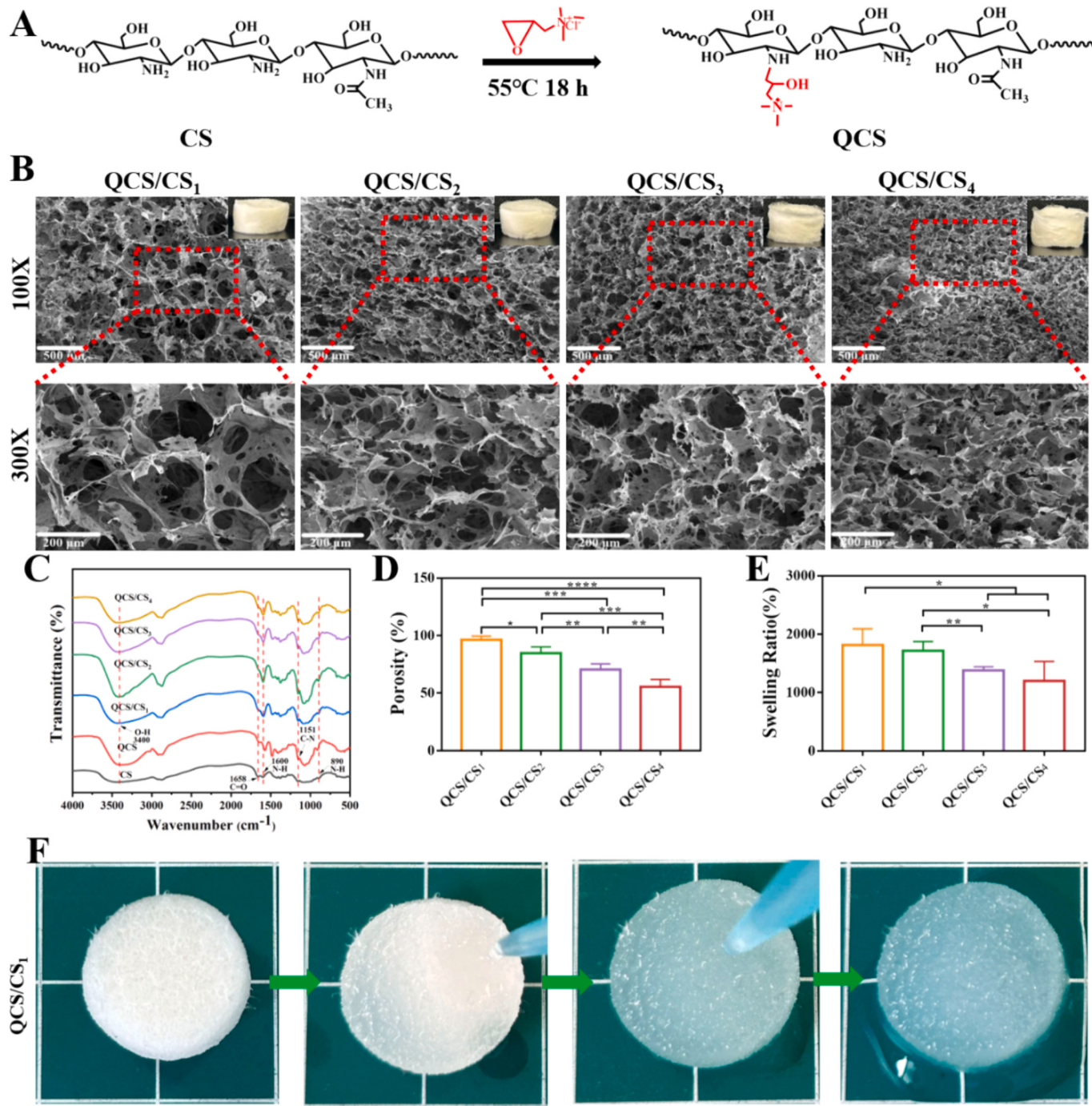


Fig. 3. Structural characterization of QCS/CS sponge. (A) Synthesis of quaternary ammonium chitosan; (B) SEM images of QCS/CS sponge; (C) FTIR spectra of CS, QCS, QCS/CS sponge; (D) Porosity of QCS/CS sponge; (E) Swelling ratio of QCS/CS sponge; (F) Optical photographs of swelling of QCS/CS sponge.

cross-linking force to promote the formation of hydrogel. It can be further seen from Fig. 1B that with the increase of CS, the color of the QCS/CS hydrogel changed from transparent to white, which is due to the increase of cross-linking sites between CS, increasing the cross-linking density of the QCS/CS hydrogel.

3.2. Self-assembly mechanism of QCS/CS hydrogel simulated by molecular dynamics

To verify our hypothesis, the state of CS in a neutral aqueous solution was simulated using molecular dynamics. After applying a force field, CS molecules rapidly aggregate in neutral aqueous solution and form CS

aggregates (Fig. 2A). The number of CS aggregates formed in the final system is 18 (Fig. 2C) and the largest cluster structure consists of 8 CS molecules (Fig. 2B). Under neutral conditions, there exists strong hydrogen bond effect between CS and they are easy to form aggregates and precipitate (Mottaghitalab et al., 2024), which is reflected in the simulation result. After the introduction of QCS in the system, multiple CS-QCS and CS-CS aggregates form (Fig. 2D), which shows that QCS and CS can form a stable structure through hydrogen bonding. The number of CS-QCS and CS-CS aggregates formed in the final system is 25 (Fig. 2F), with the largest cluster structure consisting of 3 CS molecules and 1 QCS molecule (Fig. 2E). The introduction of QCS can effectively avoid the over aggregation of CS molecules after neutralizing the acidity

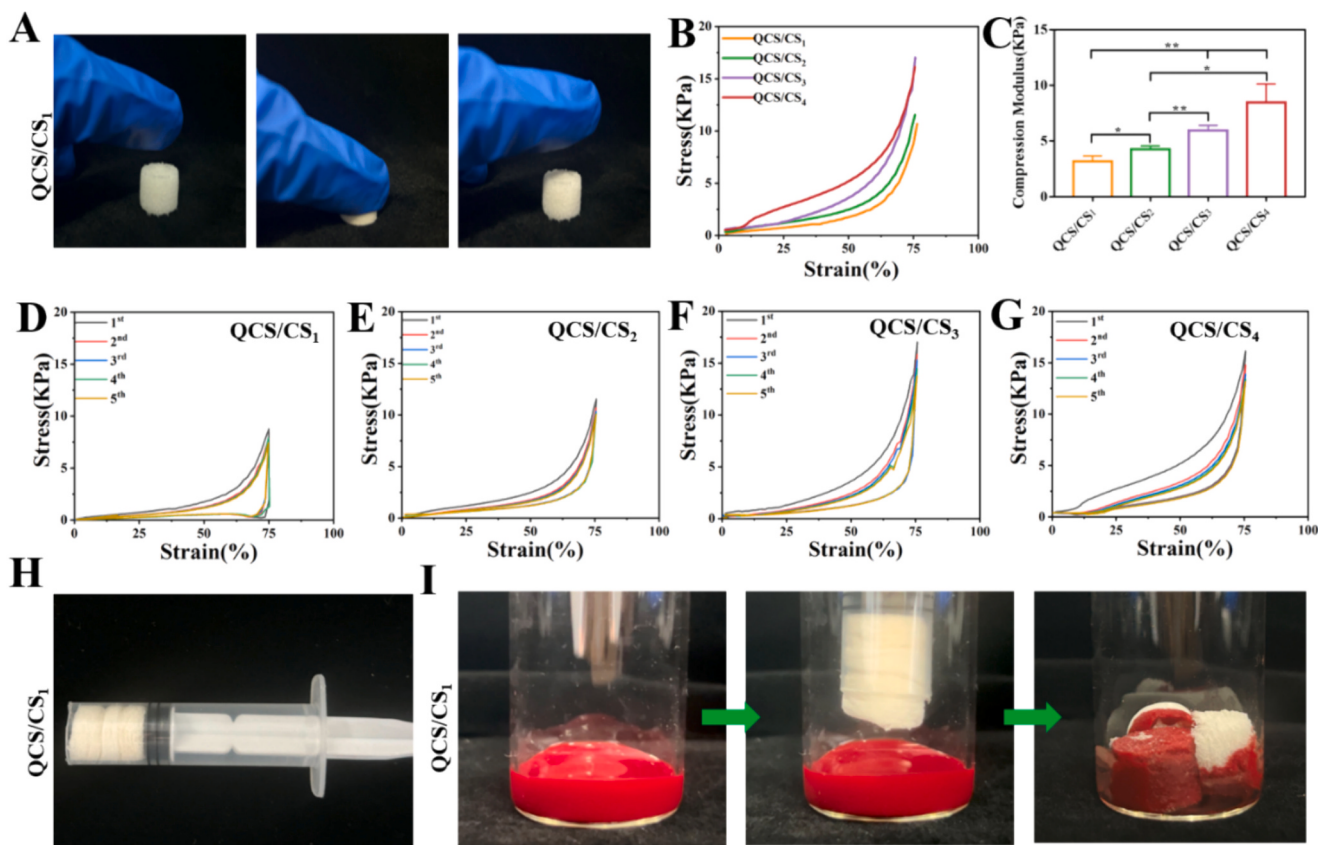


Fig. 4. Shape memory and mechanical properties of QCS/CS sponge. (A) Photographs of dried QCS/CS sponge, showing the initial state, compression state, and recovery state; (B) Stress-strain curve at compression strain of 75 %; (C) Compression modulus of QCS/CS sponge at 75 % compression; (D-G) Cyclic compressive stress-strain curves of QCS/CS sponge for 5 times; (H) Optical photograph of QCS/CS sponge after compression; (I) Picture of the compressed sponge quickly absorbs blood and recovery to its original shape.

and CS molecule can still form stable crosslinking through hydrogen bond, which verifies the hypothesis proposed in this study.

3.3. Surface morphology and chemical structure characterization of QCS/CS sponge

QCS/CS sponges have interpenetrating pore structure, as shown in Fig. 3B. With the increase of CS content, the concentration of the system increases, resulting in the decrease of the porosity of QCS/CS sponge. Moreover, it can be seen from the macroscopic diagram that the surface of QCS/CS₃ and QCS/CS₄ sponges is rough, which further proves that the increase of CS would lead to excessive crosslinking of CS in QCS/CS sponge.

It can be seen from the infrared spectrum (Fig. 3C) that compared with the infrared absorption peak of CS, the in-plane N—H vibration absorption peak of NH₂ at 1600 cm⁻¹ and the out-of-plane N—H vibration peak of NH₂ at 890 cm⁻¹ in the QCS spectrum are significantly shifted, indicating that glycidyl trimethyl ammonium chloride has successfully reacted with NH₂. The absorption peak of N—H in the amino group is slightly shifted. After the combination of QCS and CS, it can be seen that the width of N—H absorption peak in the amino group is between QCS and CS, indicating that the N—H absorption peak of the amino group in QCS and CS merged. The ¹H NMR spectrum of QCS (Fig. 1S) showed a peak at 3.10 ppm, corresponding to -N(CH₃)₃, suggesting that QCS was synthesized successfully.

It has been reported that sponge with porous structure can rapidly absorb tissue fluid to reduce the hydration effect of tissue fluid on the skin (Deng et al., 2023; P.X. Zhao et al., 2023). Meanwhile, the porous structure can promote the absorption of blood and promote the adhesion of blood cells and platelets to achieve rapid hemostasis (Chen et al.,

2022; Wang et al., 2024). Wound dressings with high porosity are conducive to the adhesion of cells, blood cells and platelets, thus to promote hemostasis and wound repair. The porosity of QCS/CS sponges decreased with the increase of CS content (Fig. 3D), which is caused by the increase of cross-linking degree of CS, and the result of porosity is consistent with the conclusion of SEM. Wound dressings with swelling properties can condense coagulation factors to enhance the hemostatic ability of the dressings. As can be seen from Fig. 3E, the swelling rate of QCS/CS sponge ranges from 1100 % to 1900 %, and the swelling rate decreases with the increase of CS content. Furthermore, it can be observed from Fig. 3F that the volume and shape of QCS/CS sponge changes little after water absorption, indicating that the prepared sponge has good stability.

3.4. Shape memory and mechanical properties of QCS/CS sponge

Since the sponge is required to quickly absorb water/blood and restore its original shape while maintaining its structural integrity after transported to the deep wound, mechanical stability and dynamic recoverability are particularly important for the expansibility of sponge (Ahmad et al., 2024; Li et al., 2023; Y.S. Li et al., 2024). As can be seen from Fig. 4A, the QCS/CS₁ sponges can recover to its original shape after compression. In addition, as seen in Movies S1-S4, QCS/CS₁ and QCS/CS₂ sponges immediately returned to their original shape after compression, indicating that the prepared QCS/CS sponges have good shape memory properties. However, QCS/CS₃ and QCS/CS₄ sponges did not return to their original state. Which is due to the fact that the stable crosslinked structure increases with the CS concentration increase. The stable crosslinked structure is difficult to recover after breaking in compression process. Furthermore, compression-strain tests were

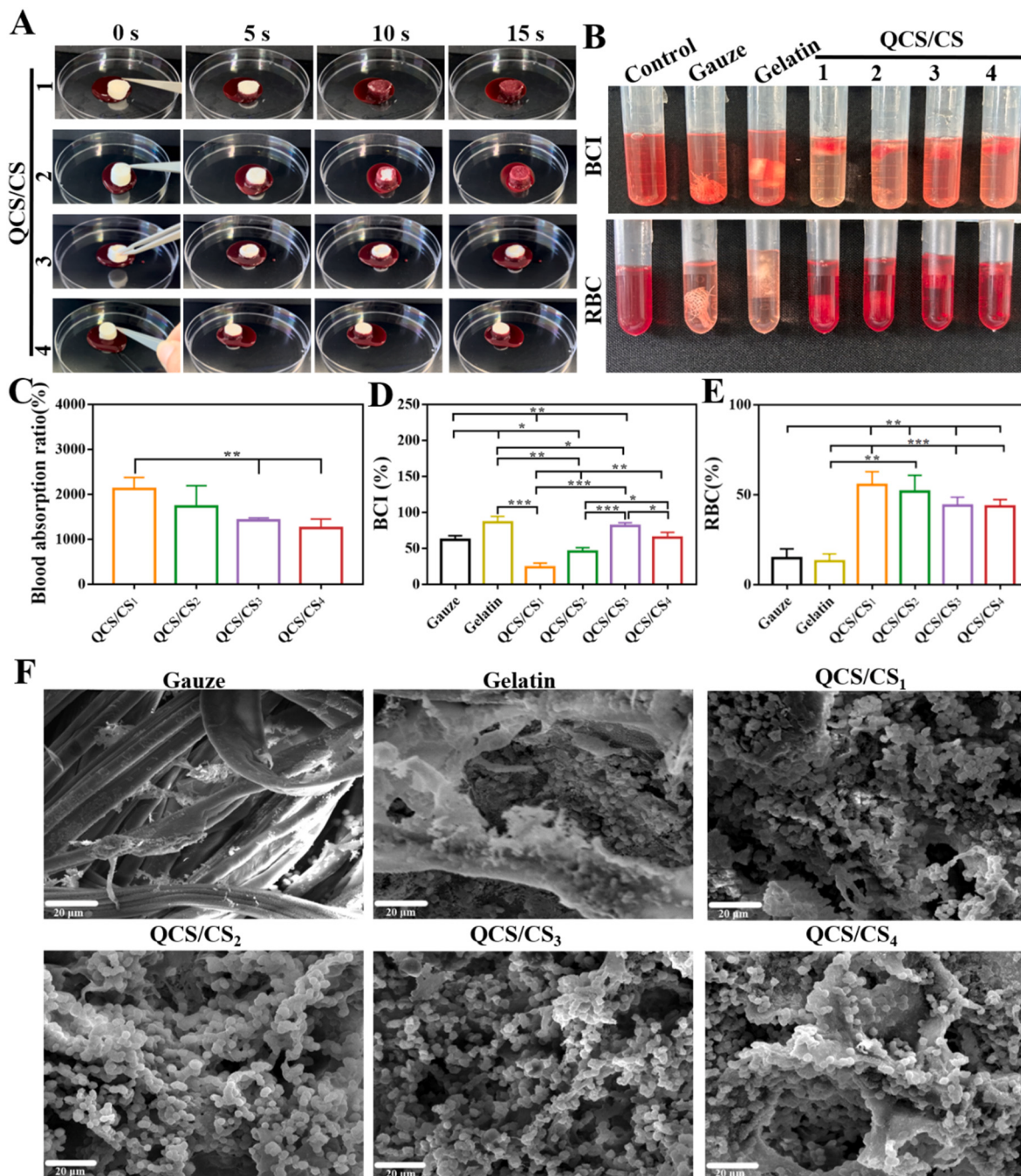


Fig. 5. *In vitro* hemostatic performance of QCS/CS sponge. (A) Four groups of sponges absorbing blood at different times; (B) Images of the BCI and RBC; (C) Blood adsorption rate; (D) BCI; (F) SEM images of blood cells adhered on gauze, gelatin sponge, QCS/CS sponge.

performed on QCS/CS sponges to evaluate their mechanical stability with a maximum strain of 75 %. It can be seen from Fig. 4B and C that the compression stress of the QCS/CS sponges gradually increase, which is due to the increase of CS, improving the mechanical properties of the sponge. The sponges were compressed for five times under maximum strain of 75 %, and the results showed that the recovery of QCS/CS₁ sponge obvious and the sponge exhibits good compression elasticity. In addition, the blood-sucking expansion ability of QCS/CS₁ sponge was tested after compression *in vitro* (Fig. 4H). The compressed QCS/CS sponge was placed in a syringe and then injected into a container with anticoagulant blood. The results showed that the sponge can quickly absorbed blood and returned to its original shape (Fig. 4I), indicating that the prepared QCS/CS sponge has potential advantages in the

treatment of deep wound bleeding.

3.5. *In vitro* hemostatic performance of QCS/CS sponge

The prepared QCS/CS sponges were placed in 2 mL blood for 0, 5, 10, and 15 s to observe the ability to absorb blood respectively. As can be seen from Fig. 5A, the blood absorbing rate of QCS/CS₁ and QCS/CS₂ was slightly higher than that of QCS/CS₃ and QCS/CS₄, which is caused by the degree of cross-linking in each group. Furthermore, the hemostatic ability of QCS/CS sponge was evaluated by blood clotting index (BCI) and blood cell adhesion rate (RBC). In the BCI test, after the water was added into the test tube, the uncoagulated red blood cells will burst, exposing hemoglobin to the water and causing the solution turn red. So,

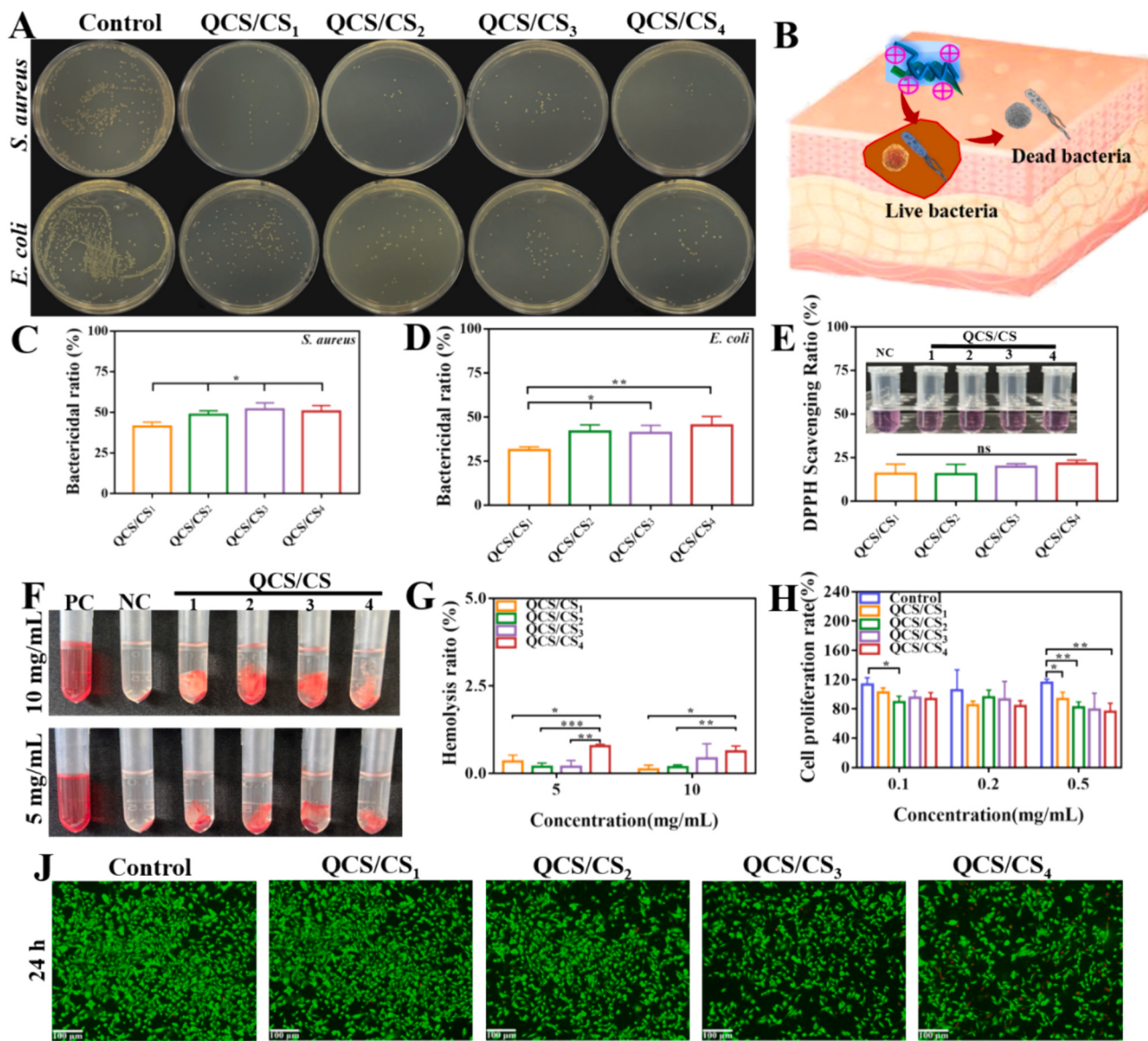


Fig. 6. Antibacterial, antioxidant property and biocompatibility of QCS/CS sponge. (A) Images of bacterial colonies formed by *S. aureus* and *E. coli* treated with control and QCS/CS sponge; (B) Antibacterial diagram of QCS/CS sponge; (C)The bacterial ratio of *S. aureus* and (D) *E. coli* treated with different sponge; (E) DPPH scavenging ratio of QCS/CS sponge; (F) Images of the *in vitro* hemolysis; (G) Hemolysis ratio; (H) Cell proliferation of 3 T3 cells incubated in sponge extracts with different concentration for 24 h; (J) Live/dead staining pictures of 3 T3 cells cultured on QCS/CS sponge extracts for 24 h.

the higher the number of uncoagulated red blood cells, the darker the solution. The clotting ability of the sponge is judged by the color of the solution. And darker color means worse clotting ability. As can be seen from Fig. 5B, the color of the QCS/CS group is lighter compared with gauze group and gelatin group, and the color of the QCS/CS₁ group is the lightest. Furthermore, it can also be seen from the results of the BCI (Fig. 5D) that QCS/CS₁ group has low BCI, which indicates that QCS/CS₁ group has excellent coagulation effect. In addition, the RBC (Fig. 5E) was above 40 %, which was significantly higher than gauze and gelatin sponge.

The blood cell adhesion of QCS/CS sponge was further evaluated. Fig. 5F showed the adhesion morphology of blood cells on the surface of the sponge. As the results showed, the blood cell adhesion in gauze is few and increases slightly in gelatin group. The QCS/CS₁ sponge had large number of blood cell aggregate in the porous network, which is due to the large and porous network structure. The QCS/CS sponges can rapidly bind water and blood cells in the blood, and the positively charged QCS can bind to blood cells by electric charge to promote blood

cell adhesion. These results indicated that QCS/CS₁ sponges had excellent hemostatic effect.

3.6. Antibacterial, antioxidant property and biocompatibility of QCS/CS sponge

After damaged, the skin loses its function of barrier protection, which makes the wound vulnerable to bacterial attack (Wang et al., 2024). Therefore, the hemostatic sponge should have good antibacterial property to protect the wound from external bacterial infection, accelerating the wound healing. It can be seen from Fig. 6A that compared with control group, QCS/CS sponges showed good antibacterial properties (Fig. 6B). The bacteriostatic rate of each sponge was further tested. As shown in Fig. 6C and D, the results indicate that all the QCS/CS sponges had great antibacterial property. Due to the introduction of QCS, the positive charge on the surface of QCS/CS sponges interacted with the negative charge on the surface of the bacteria, resulting in the death of the bacteria.

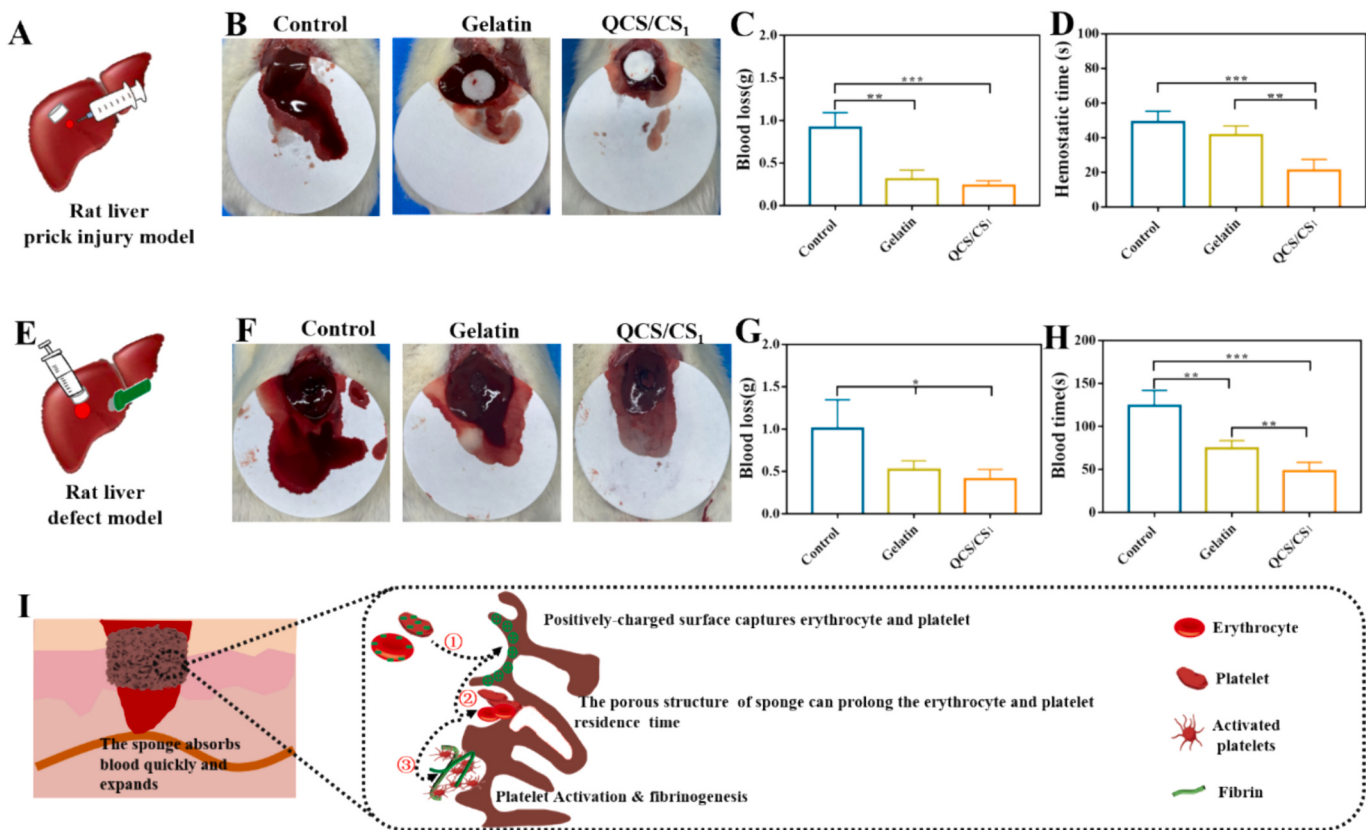


Fig. 7. Hemostatic performance of QCS/CS sponge *in vivo*. (A) Schematic representation of rat liver defect model; (B) Images of hemostasis in rat liver prick injury model by use of control, gelatin sponge and QCS/CS sponge; (C) Blood loss; (D) Hemostatic time; (E) Schematic representation of liver volume defect model; (F) Images of hemostasis in rat liver volume defect model by use of control, gelatin sponge and QCS/CS sponge; (G) Blood loss; (H) Hemostatic time; (I) Schematics diagram of hemostatic mechanism of the porous QCS/CS sponges.

Damaged wound would produce a large number of oxygen free radicals, which can lead to sustained oxidative stress and damage cells, hindering the process of wound healing (Liu et al., 2024; Pranantyo et al., 2024). Therefore, hemostatic sponge also needs free radical scavenging ability to accelerate wound healing. The free radical scavenging capacity of QCS/CS sponges was evaluated by DPPH scavenging test. As shown in Fig. 6E, compared with the control group, all the QCS/CS groups were slightly lighter in color, indicating that the QCS/CS sponges had free radical scavenging ability. The DPPH scavenging rates of the QCS/CS sponges were $(15.62 \pm 5.59)\%$, $(15.55 \pm 5.55)\%$, $(19.64 \pm 1.83)\%$ and $(21.43 \pm 1.99)\%$, respectively. The results showed that QCS/CS sponges have antioxidant properties because quaternary ammonium salts can interfere with the hydrogen bond network between hydroxyl and amine groups and thus have the ability to scour free radicals (Andreica et al., 2023).

The hemolysis rate of QCS/CS sponge with different concentration (5 and 10 mg/mL) was tested (Fig. 6F). The hemolysis rate of all the QCS/CS sponge group at different concentrations was $<5\%$ (Fig. 6G), indicating that the QCS/CS sponge has good blood compatibility and meets the requirement as hemostatic agents. In addition, the cytocompatibility of QCS/CS sponges was further evaluated. As shown in Fig. 6H, the extract liquid of QCS/CS sponge with different concentration was co-cultured with cell. The results show that the cell proliferation rate of the prepared sponge with concentration less than or equal to 0.5 mg/mL is $>70\%$, showing good cytocompatibility. In addition, live/dead staining was also used to evaluate the cytotoxicity of the sponge. The positive charge of the QCS would react with the negative charge on the cell surface, resulting in a small amount of cell death. Therefore, when the concentration of the sponge extract was 0.5 mg/mL, most of the cells are alive and only small amount of dead cells exist (Fig. 6H). It also can

be seen from the Fig. 6J that the number of cells in QCS/CS₃ and QCS/CS₄ groups decreased compared with other groups. The aggregation of CS in QCS/CS₃ and QCS/CS₄ was greater than other groups, weakening the cross-linking between CS and QCS. The instability of the prepared sponge results in the leaching of QCS, further leading to the cell death (Xu et al., 2023; Zhao, Tian, et al., 2023). In conclusion, the prepared QCS/CS₁ sponge had good biocompatibility and can satisfy the application of hemostasis.

3.7. Hemostasis performance *in vivo* of QCS/CS sponge

QCS/CS₁ sponge presented good antibacterial ability, blood coagulation property and biocompatibility through *in vitro* experiments, showing its potential as an ideal material for rapid hemostasis and wound healing promotion. Therefore, *in vivo* evaluation of the hemostatic performance of the cryogenic solution was further performed using rat liver prick injury model and rat liver defect model. The hemostatic capacity of QCS/CS sponge *in vivo* was assessed by blood loss in rat liver prick injury model (Fig. 7A and B). As shown in Fig. 7C and D, the blood loss of QCS/CS₁ sponge group (0.23 ± 0.057) g was lower than that of blank group (0.91 ± 0.18) g and gelatin sponge group (0.31 ± 0.11) g, indicating that the hemostatic capacity of QCS/CS₁ sponge was higher than that of commercial gelatin hemostatic sponge. In addition, QCS/CS₁ sponge also has the shortest hemostatic time with only 21 s, while gelatin sponge is 42 s. A similar result was observed in rat liver defect model (Fig. 7E). As shown in Fig. 7F, the hemostatic effect of QCS/CS₁ sponge was better than that of gauze and gelatin sponge. The blood loss (Fig. 7G) in the control group (1.01 ± 0.34 g) was higher than that in the gelatin (0.57 ± 0.10 g) group and QCS/CS (0.40 ± 0.09 g) group. As shown in Fig. 7H, the maximum hemostatic time of the control

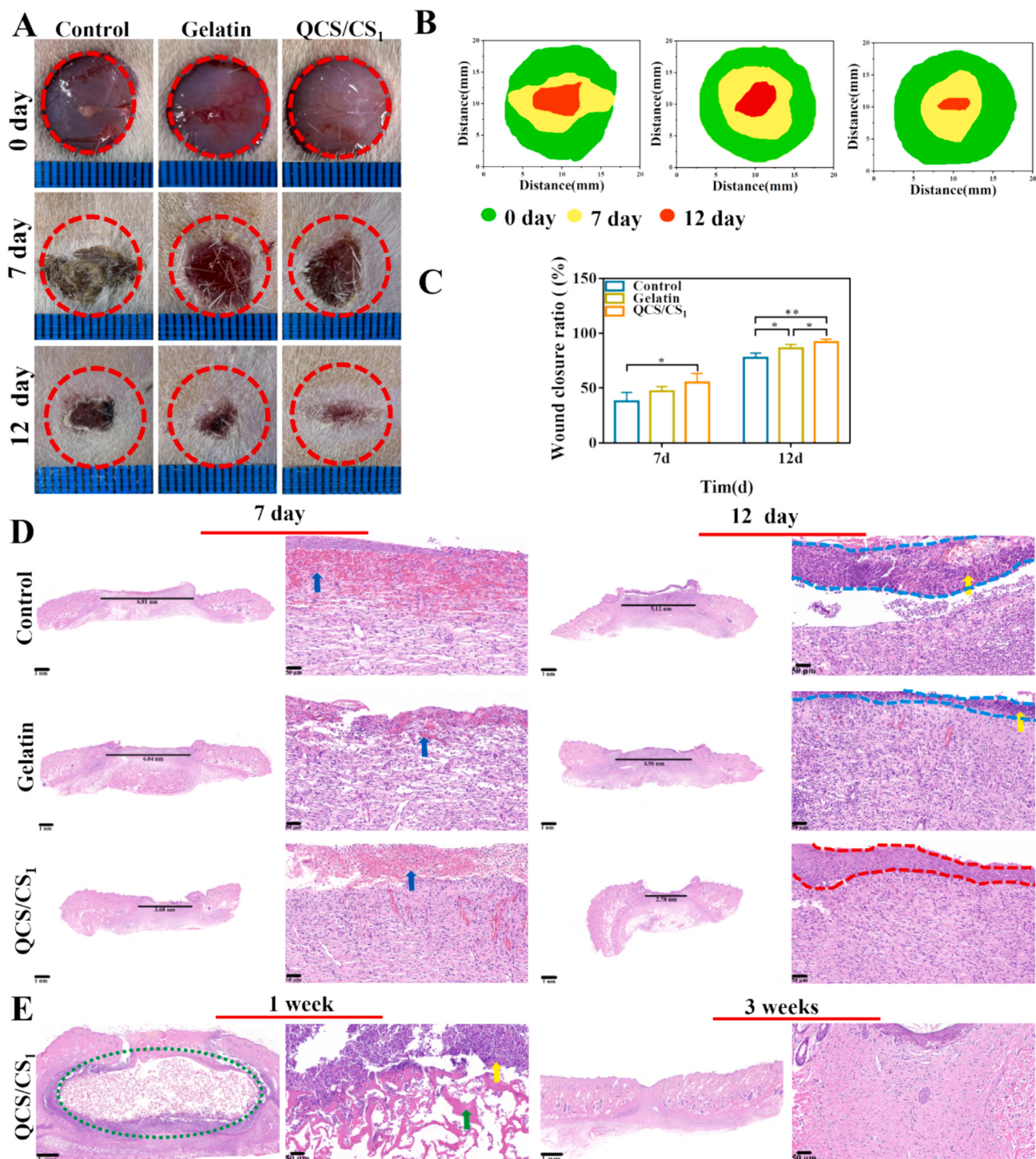


Fig. 8. *In vivo* wound healing evaluation and biosafety performance of QCS/CS sponge. (A) Photographs of wound healing in control group, gelatin sponge group and QCS/CS sponge group on 0, 7th and 12th day; (B) Simulation of wound healing with different healing times; (C) Wound closure rate with different healing time; (D) H&E stained histological images of regenerated skin tissue treated with different sponge on 7th and 12th day; (E) H&E staining of tissue sections implanted in rats with QCS/CS sponge on 1 week and 3 weeks (Green dashed ellipses and arrows represent material, yellow arrow represent inflammatory cells). (For interpretation of the references to color in this figure legend, the reader is referred to the web version of this article.)

group is (124 ± 17.96) s, while the time of QCS/CS₁ sponge shortens to (48 ± 10.23) s. The hemostatic mechanism of QCS/CS sponge was shown in Fig. 7I. Firstly, the porous structure of sponge can rapidly absorb blood and expand to fill the wound after transported into the wound, forming a physical barrier to promote hemostasis (Zhang et al., 2022). In addition, the positively charged QCS can promote the adhesion and enrichment of the negative charged erythrocyte and platelets (Liang

et al., 2023; P. Zhao et al., 2023). The porous structure of QCS/CS sponges increases the retention time of erythrocyte and platelets, and further activates platelets to promote the formation of fibrin, thus promoting the rapid coagulation of blood (Lee et al., 2024). In summary, QCS/CS sponge has great potential in the application of deep wound bleeding and is a promising hemostatic material.

3.8. In vivo full-thickness wound healing of QCS/CS sponge

The wound healing promotion of QCS/CS sponge was tested by establishing a full-thickness skin defect model in rat. As shown in Fig. 8A, the wound repair in blank, gelatin sponge and QCS/CS₁ sponge groups were observed by taking macroscopic images on the 0, 7th and 12th day, respectively. On the 7th day, significant defect was observed in the control group, and the damaged area in all groups reduced. QCS/CS₁ sponge showed the most distinguished contraction in wound area on the 7th and 12th day. The recovery rate of gelatin sponge group ($62.04 \pm 4.83\%$) and QCS/CS group ($69.63 \pm 10.48\%$) was significantly improved compared to the control group ($50.11 \pm 8.30\%$) after 7 days. On the 12th day, the wound healing rate of QCS/CS₁ group was over 90 %. These results indicate that the QCS/CS₁ sponge has better effect in promoting skin wound healing. Most sponge dressings tend to adhere to the wound after long-term contact with the wound, which is easy to cause secondary damage when removed. The prepared QCS/CS₁ sponge in this study has the advantage of on-demand stripping (Fig. S2). The QCS/CS₁ sponge was prepared by physical cross-linking induced by hydrogen bond. Under the action of acetic acid in low concentration, the amino group in the QCS/CS₁ sponge network was protonated, and the hydrogen bond effect was reduced greatly. So the surface of the sponge dissolved quickly, and the sponge can be easily detached from the wound. QCS/CS sponge with porous structure can rapidly absorb tissue fluid to reduce the hydration effect of tissue fluid on the skin. In addition, the QCS/CS sponges exhibit good hemostatic properties and antibacterial capabilities, offering a significant advantage in wound care and hemostasis. The QCS/CS sponges are physically crosslinked and can be dissolved quickly under the action of acetic acid of low concentration, which allows the sponge to be peeled off on demand. Therefore, the prepared QCS/CS sponges hold promising prospects for application in preventing wound infection and rapid hemostasis.

The wound regeneration effect was further evaluated by H&E staining. As shown in Fig. 8D, there was only a small amount of new granulation tissue existing, and a large number of inflammatory cells can be seen in the blank group on the 7th day. The fibroblasts are sparse and a few new capillaries are disorganized. QCS/CS₁ group had fewer inflammatory cells and denser granulation tissue formation. On the 12th day, compared with the control group, complete collagen fibers began to appear in the QCS/CS₁ group, and the tissue formation was dense and orderly.

QCS/CS₁ sponge was implanted into the subcutaneous tissue in the back of rats to observe the degradation. As can be seen in Fig. 8E, there was a large amount of undegraded sponge (green dashed ellipse) and inflammatory cells (yellow arrow) appearing in the surrounding t after implantation for 7th day. On the 21th day, it can be observed from H&E staining that the sponge had been basically degraded, and no obvious pathological reactions appeared in the tissue, indicating that the QCS/CS₁ sponge had good biodegradability. Therefore, QCS/CS sponge can promote wound repair as well as good biocompatibility and biodegradability, which a promising material for wound repair.

4. Conclusion

In summary, an injectable and expandable QCS/CS sponge was prepared for the hemostasis of deep wound and wound healing. Compared with traditional preparation method, the QCS/CS sponge was constructed by CS and QCS self-assembly without acid retention and chemical crosslinker introduction. QCS can form hydrogen bond with CS to reduce the effect of intermolecular hydrogen bond of CS to avoid precipitation. By regulating the ratio of QCS to CS, the stable QCS/CS₁ sponge was selected. The QCS/CS₁ sponge exhibits expansibility and water/blood triggered shape memory property. Meanwhile, it exhibits good antibacterial property, which can protect the wound from bacterial invasion. The simple and green preparation method is an efficient way to prepare expandable chitosan-based sponge for hemostasis and wound

healing.

Supplementary data to this article can be found online at <https://doi.org/10.1016/j.carbpol.2024.122699>.

CRediT authorship contribution statement

Shujun Cao: Conceptualization, Investigation, Data curation, Formal analysis, Writing – original draft, Funding acquisition. **Peihong Ji:** Investigation, Data curation, Formal analysis. **Lili Hao:** Software, Validation, Funding acquisition. **Chao Sun:** Resources, Funding acquisition, Writing - review & editing. **Hongli Mao:** Conceptualization, Resources, Funding acquisition, Project administration, Supervision, Writing - review & editing. **Zhongwei Gu:** Supervision, Writing - review & editing.

Declaration of competing interest

The authors declare no conflict of interest.

Data availability

Data will be made available on request.

Acknowledgments

This work was financially supported by the National Natural Science Foundation of China (32271467, 32301246), the Natural Science Foundation of Jiangsu Province (BK20230315), the Priority Academic Program Development of Jiangsu Higher Education Institutions (PAPD), the Postdoctoral Fellowship Program of CPSF (GZC20240697), and the Jiangsu Funding Program for Excellent Postdoctoral Talent.

References

- Ahmad, K. Z., Younus, W. M., Aijaz, A., et al. (2024). Multifunctional chitosan-cross linked-curcumin-tannic acid biocomposites disrupt quorum sensing and biofilm formation in pathogenic bacteria [J]. *International Journal of Biological Macromolecules*, 271, Article 132719. <https://doi.org/10.1016/j.ijbiomac.2024.132719>
- Andreica, B. I., Anisiei, A., Rosca, I., et al. (2023). Quaternized chitosan-based nanofibers with strong antibacterial and antioxidant activity designed as ecological active food packaging[J]. *Food Packaging Shelf*, 39, Article 101157. <https://doi.org/10.1016/j.fpsl.2023.101157>
- Cao, S. J., Xu, G., Li, Q. J., et al. (2022). Double crosslinking chitosan sponge with antibacterial and hemostatic properties for accelerating wound repair[J]. *Composites Part B: Engineering*, 234. <https://doi.org/10.1016/j.compositesb.2022.109746>
- Cao, S. J., Bi, Z. J., Li, Q. J., et al. (2023a). Shape memory and antibacterial chitosan-based cryogel with hemostasis and skin wound repair[J]. *Carbohydrate Polymers*, 305, 109746. <https://doi.org/10.1016/j.carbpol.2023.120545>
- Cao, S. J., Zhang, K., Li, Q. J., et al. (2023b). Injectable and photothermal antibacterial bacterial cellulose cryogel for rapid hemostasis and repair of irregular and deep skin wounds[J]. *Carbohydrate Polymers*, 320, Article 121239. <https://doi.org/10.1016/j.carbpol.2023.121239>
- Chen, J. T., Huang, Z. H., Zhang, H. Q., et al. (2022). Three-dimensional layered nanofiber sponge with in situ grown silver-metal organic framework for enhancing wound healing[J]. *Chemical Engineering Journal*, 443, Article 136234. <https://doi.org/10.1016/j.cej.2022.136234>
- Deng, S. Y., Huang, Y. G., Hu, E. L., et al. (2023). Chitosan/silk fibroin nanofibers-based hierarchical sponges accelerate infected diabetic wound healing via a HClO self-producing cascade catalytic reaction[J]. *Carbohydrate Polymers*, 321, Article 121340. <https://doi.org/10.1016/j.carbpol.2023.121340>
- Jin, Y., Wang, C., Xia, Z., et al. (2023). Photodynamic chitosan sponges with dual instant and enduring bactericidal potency for treating skin abscesses[J]. *Carbohydrate Polymers*, 306, Article 120589. <https://doi.org/10.1016/j.carbpol.2023.120589>
- Juan, L. T., Lin, S. H., Wong, C. W., et al. (2022). Functionalized cellulose nanofibers as Crosslinkers to produce chitosan self-healing hydrogel and shape memory Cryogel [J]. *ACS Applied Materials & Interfaces*, 14(32), 36353–36365. <https://doi.org/10.1021/acsmami.2c07170>
- Lee, V. K., Lee, T., Ghosh, A., et al. (2024). An architecturally rational hemostat for rapid stopping of massive bleeding on anticoagulation therapy[J]. *Proceedings of the National Academy of Sciences of the United States of America*, 121(5), Article e2316170121. <https://doi.org/10.1073/pnas.2316170121>
- Li, Y., Yang, Z. F., Sun, Q., et al. (2023). Biocompatible Cryogel with good breathability, exudate management, antibacterial and immunomodulatory properties for infected diabetic wound healing[J]. *Advanced Science*, 10(31), 202304243. <https://doi.org/10.1002/advs.202304243>

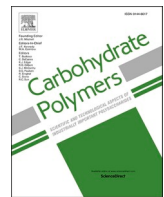
- Li, Y. S., Chu, C. N., Chen, C. T., et al. (2024). Quaternized chitosan/oxidized bacterial cellulose cryogels with shape recovery for noncompressible hemorrhage and wound healing[J]. *Carbohydrate Polymers*, 327, Article 121679. <https://doi.org/10.1016/j.carbpol.2023.121679>
- Li, Z. T., Xing, X. L., Zhao, C. R., et al. (2024). A rapid interactive chitosan-based medium with antioxidant and pro-vascularization properties for infected burn wound healing [J]. *Carbohydrate Polymers*, 333, Article 121991. <https://doi.org/10.1016/j.carbpol.2024.121991>
- Liang, Z., Luo, J. L., Liu, S. M., et al. (2023). Injectable, antibacterial, ROS scavenging and pro-angiogenic hydrogel adhesives promote chronic wound healing in diabetes via synergistic release of NMN and Mg²⁺[J]. *Chemical Engineering Journal*, 475, Article 146092. <https://doi.org/10.1016/j.cej.2023.146092>
- Liu, X., Sun, Y., Wang, J., et al. (2024). A tough, antibacterial and antioxidant hydrogel dressing accelerates wound healing and suppresses hypertrophic scar formation in infected wounds[J]. *Bioactive Materials*, 34, 269–281. <https://doi.org/10.1016/j.bioactmat.2023.12.019>
- Liu, Y., Niu, H., Wang, C., et al. (2022). Bio-inspired, bio-degradable adenosine 5'-diphosphate-modified hyaluronic acid coordinated hydrophobic undecanal-modified chitosan for hemostasis and wound healing[J]. *Bioactive Materials*, 17, 162–177. <https://doi.org/10.1016/j.bioactmat.2022.01.025>
- Liu, Z. C., Xu, Y. Z., Su, H. N., et al. (2023). Chitosan-based hemostatic sponges as new generation hemostatic materials for uncontrolled bleeding emergency: Modification, composition, and applications[J]. *Carbohydrate Polymers*, 311, Article 120780. <https://doi.org/10.1016/j.carbpol.2023.120780>
- Liu, B. T., Hu, E. L., Xie, R. Q., et al. (2022). Microcluster colloidosomes for hemostat delivery into complex wounds: A platform inspired by the attack action of torpedoes [J]. *Bioactive Materials*, 16, 372–387. <https://doi.org/10.1016/j.bioactmat.2022.01.002>
- Luo, Y., Cui, L., Zou, L., et al. (2022). Mechanically strong and on-demand dissolvable chitosan hydrogels for wound dressing applications[J]. *Carbohydrate Polymers*, 294, Article 119774. <https://doi.org/10.1016/j.carbpol.2022.119774>
- Marani, R. S., & Ehtesabi, H. (2023). A flexible and hemostatic chitosan, polyvinyl alcohol, carbon dot nanocomposite sponge for wound dressing application[J]. *International Journal of Biological Macromolecules*, 224, 831–839. <https://doi.org/10.1016/j.ijbiomac.2022.10.169>
- Mottaghitalab, F., Yazdi, M. K., Saeb, M. R., et al. (2024). Green and sustainable hydrogels based on quaternized chitosan to enhance wound healing [J]. *Chemical Engineering Journal*, 492, Article 152288. <https://doi.org/10.1016/j.cej.2024.152288>
- Peng, W., Liu, C., Lai, Y. J., et al. (2023). An adhesive/anti-adhesive Janus tissue patch for efficient closure of bleeding tissue with inhibited postoperative adhesion[J]. *Advanced Science*, 10(21), Article 2301427. <https://doi.org/10.1002/advs.202301427>
- Pranantyo, D., Yeo, C. K., Wu, Y., et al. (2024). Hydrogel dressings with intrinsic antibiofilm and antioxidative dual functionalities accelerate infected diabetic wound healing[J]. *Nature Communications*, 15(1), 954. <https://doi.org/10.1038/s41467-024-44968-y>
- Priddy-Arrington, T. R., Edwards, R. E., Colley, C. E., et al. (2023). Characterization and optimization of injectable in situ crosslinked chitosan-genipin hydrogels[J]. *Macromolecular Bioscience*, 23(6), Article 202200505. <https://doi.org/10.1002/mabi.202200505>
- Qi, L. H., Mu, L. X., Guo, X. J., et al. (2023a). Fast expandable chitosan-fibers Cryogel from ambient drying for noncompressible bleeding control and in situ tissue regeneration[J]. *Advanced Functional Materials*, 33(16), 202212231. <https://doi.org/10.1002/adfm.202212231>
- Qi, L. H., Wang, S., Chen, L., et al. (2023b). Bioinspired multiscale Micro-/nanofiber network design enabling extremely compressible, fatigue-resistant, and rapidly shape-recoverable Cryogels[J]. *ACS Nano*, 17(7), 6317–6329. <https://doi.org/10.1021/acsnano.2c10462>
- Qiao, L. P., Liang, Y. P., Chen, J. Y., et al. (2023). Antibacterial conductive self-healing hydrogel wound dressing with dual dynamic bonds promotes infected wound healing[J]. *Bioactive Materials*, 30, 129–141. <https://doi.org/10.1016/j.bioactmat.2023.07.015>
- Wang, J. X., He, J. H., Yang, Y. T., et al. (2024). Hemostatic, antibacterial, conductive and vascular regenerative integrated cryogel for accelerating the whole wound healing process[J]. *Chemical Engineering Journal*, 479, Article 147577. <https://doi.org/10.1016/j.cej.2023.147577>
- Wang, X. Y., Wang, J., Zhao, C. X., et al. (2023). Facile fabrication of chitosan colloidal films with pH-tunable surface hydrophobicity and mechanical properties[J]. *Food Hydrocolloids*, 137, Article 108429. <https://doi.org/10.1016/j.foodhyd.2022.108429>
- Xu, X., Zeng, Y. B., Chen, Z., et al. (2023). Chitosan-based multifunctional hydrogel for sequential wound inflammation elimination, infection inhibition, and wound healing[J]. *International Journal of Biological Macromolecules*, 235, Article 123847. <https://doi.org/10.1016/j.ijbiomac.2023.123847>
- Yang, X. X., Wang, C. W., Liu, Y. H., et al. (2021). Inherent antibacterial and instant swelling e-poly-lysine/poly(ethylene glycol) Diglycidyl ether superabsorbent for rapid hemostasis and bacterially infected wound healing[J]. *ACS Applied Materials & Interfaces*, 13(31), 36709–36721. <https://doi.org/10.1021/acsami.1c02421>
- Yao, L. T., Gao, H. C., Lin, Z. F., et al. (2022). A shape memory and antibacterial cryogel with rapid hemostasis for noncompressible hemorrhage and wound healing[J]. *Chemical Engineering Journal*, 428, Article 131005. <https://doi.org/10.1016/j.cej.2021.131005>
- Zhang, S. X., Lei, X. X., Lv, Y. L., et al. (2024). Recent advances of chitosan as a hemostatic material: Hemostatic mechanism, material design and prospective application[J]. *Carbohydrate Polymers*, 327, Article 121673. <https://doi.org/10.1016/j.carbpol.2023.121673>
- Zhang, Y. P., Wang, Y., Chen, L., et al. (2022). An injectable antibacterial chitosan-based cryogel with high absorbency and rapid shape recovery for noncompressible hemorrhage and wound healing[J]. *Biomaterials*, 285, Article 121546. <https://doi.org/10.1016/j.biomaterials.2022.121546>
- Zhao, P., Zhang, Y., Chen, X., et al. (2023). Versatile hydrogel dressing with skin adaptiveness and mild Photothermal antibacterial activity for methicillin-resistant staphylococcus aureus-infected dynamic wound healing[J]. *Advanced Science*, 10 (11), Article 202206585. <https://doi.org/10.1002/advs.202206585>
- Zhao, P. X., Feng, Y., Zhou, Y. Q., et al. (2023). Gold@Halloysite nanotubes-chitin composite hydrogel with antibacterial and hemostatic activity for wound healing[J]. *Bioactive Materials*, 20, 355–367. <https://doi.org/10.1016/j.bioactmat.2022.05.035>
- Zhao, X., Huang, Y., Li, Z. L., et al. (2024). Injectable self-expanding/self-propelling hydrogel adhesive with Procoagulant activity and rapid gelation for lethal massive hemorrhage management[J]. *Advanced Materials*, 3208701. <https://doi.org/10.1002/adma.202308701>
- Zhao, X., Liang, Y. P., Guo, B. L., et al. (2021). Injectable dry cryogels with excellent blood-sucking expansion and blood clotting to cease hemorrhage for lethal deep-wounds, coagulopathy and tissue regeneration[J]. *Chemical Engineering Journal*, 403, Article 126329. <https://doi.org/10.1016/j.cej.2020.126329>
- Zhao, Y. N., Tian, C., Liu, Y. M., et al. (2023). All-in-one bioactive properties of photothermal nanofibers for accelerating diabetic wound healing[J]. *Biomaterials*, 295, Article 122029. <https://doi.org/10.1016/j.biomaterials.2023.122029>

Update

Carbohydrate Polymers

Volume 353, Issue , 1 April 2025, Page

DOI: <https://doi.org/10.1016/j.carbpol.2025.123293>



Corrigendum

Corrigendum to “Self-assembling chitosan based injectable and expandable sponge with antimicrobial property for hemostasis and wound healing” [Carbohydr. Polym. 347 (2025) 122699]



Shujun Cao ^a, Peihong Ji ^a, Lili Hao ^a, Chao Sun ^{b,*}, Hongli Mao ^{a,*}, Zhongwei Gu ^a

^a Research Institute for Biomaterials, Tech Institute for Advanced Materials, Bio-inspired Biomedical Materials & Devices Center, College of Materials Science and Engineering, Jiangsu Collaborative Innovation Center for Advanced Inorganic Function Composites, Suqian Advanced Materials Industry Technology Innovation Center, Nanjing Tech University, Nanjing 211816, China

^b Department of Spine Surgery, The Affiliated Jiangning Hospital of Nanjing Medical University, Nanjing 211100, China

The authors regret in the cell live/dead staining images (Fig. 6J), a mistake was made in the final combination process of picture that using

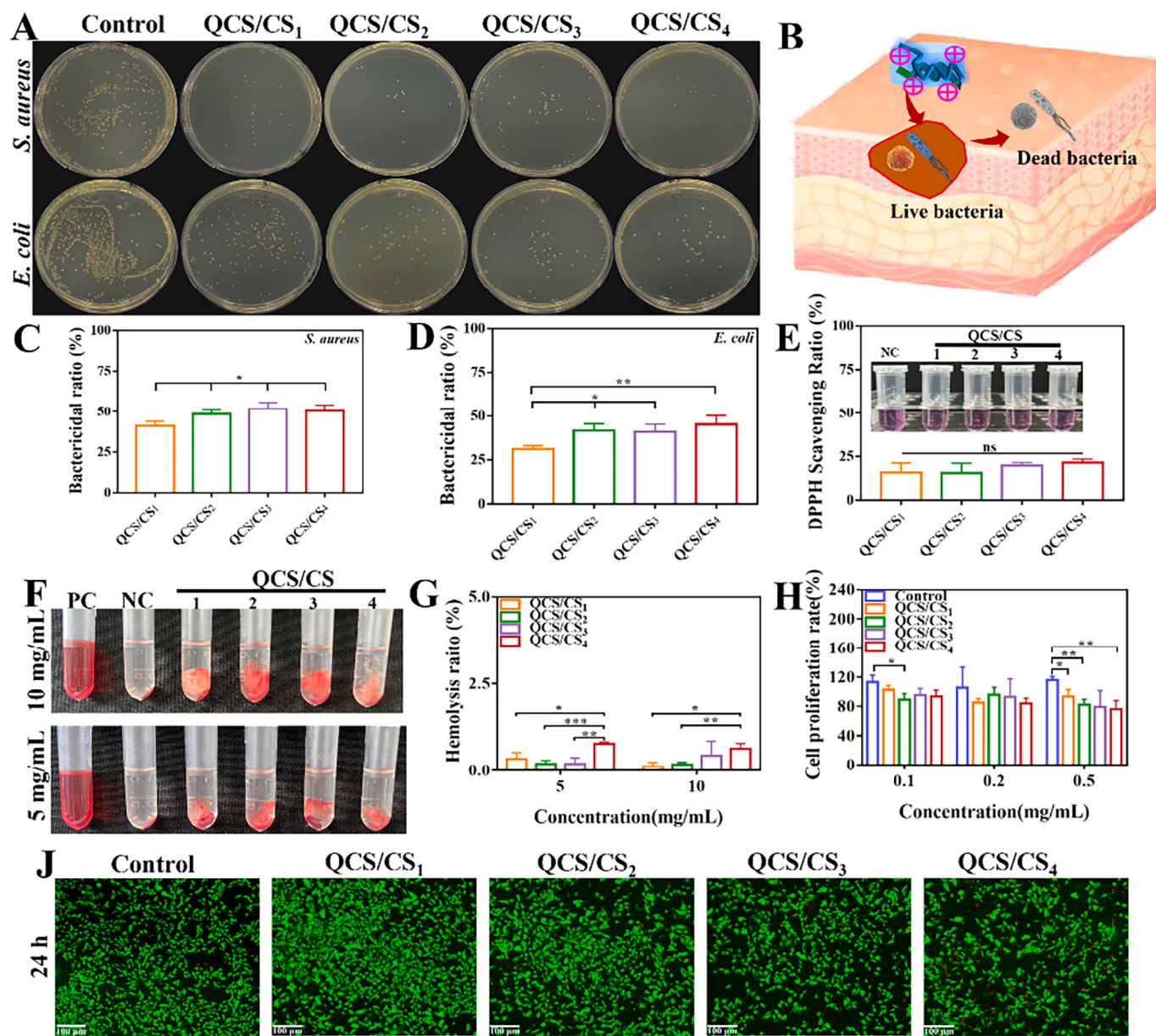
the same images for the control group and QCS/CS1 group.

The corrected Fig. 6 is as follows:

DOI of original article: <https://doi.org/10.1016/j.carbpol.2024.122699>.

* Corresponding authors.

E-mail addresses: drsunchao@163.com (C. Sun), h.mao@njtech.edu.cn (H. Mao).



The authors would like to apologise for any inconvenience caused.